A haemodynamic network involving the insula, the cingulate, and the basal forebrain correlates with EEG synchronization phases of sleep instability

Vasileios Kokkinos[1,2,4], Serge Vulliémoz[3,7], Andreas M. Koupparis[4,8], Michalis Koutroumanidis[5,6], George K. Kostopoulos[4], Louis Lemieux[3], Kyriakos Garganis[2]

[1]Department of Neurological Surgery, School of Medicine, University of Pittsburgh, PA, USA.

[2]Epilepsy Center of Thessaloniki, St. Luke's Hospital, Thessaloniki, Greece.

[3]Department of Clinical and Experimental Epilepsy, UCL Institute of Neurology, Queen Square, London, UK and MRI Unit, Epilepsy Society, Chalfont St. Peter, UK.

[4]Neurophysiology Unit, Department of Physiology, Medical School, University of Patras, Greece.

[5]Department of Clinical Neurophysiology and Epilepsies, Guy's, St. Thomas' and Evelina Hospital for Children, NHS Foundation Trust, London, UK.

[6]Department of Neuroscience, Institute of Psychiatry, Kings College London, UK.

[7]EEG and Epilepsy Unit, Neurology, University Hospital and Faculty of Medicine, Geneva, Switzerland.

[8]Montreal Neurological Institute, McGill University, Montreal, Canada.

Corresponding author: Vasileios Kokkinos, Department of Neurological Surgery, University of Pittsburgh, 15213, PA, USA. email: vasileios.kokkinos@pitt.edu

Abstract

The cyclic alternating pattern (CAP) encompasses the pseudo-periodic appearance of synchronized brain waves and rhythms and is considered a regulator of the NREM sleep vigilance level, reflecting sleep instability. To determine the brain regions responsible for this phenomenon, we scored and analyzed sleep fMRI data acquired with simultaneous EEG (EEG-fMRI). Group analysis revealed a set of brain areas showing statistically significant blood oxygen-level dependent (BOLD) signal correlated positively with the synchronization phase of the CAP, most prominent being the insula, the middle cingulate gyrus, and the basal forebrain. These areas may form a network acting as a synchronization pacemaker, controlling the level of NREM sleep vigilance and the sleeper's arousability.

Keywords: EEG-fMRI | cyclic alternating pattern | sleep | insula | cingulate | basal forebrain.

Statement of Significance

The cyclic alternating pattern (CAP) is an expression of the magnitude of sleep instability, manifesting as pseudo-periodic EEG synchronization phases, providing adaptation to environmental stimuli for the purpose of defense against perturbations. Our study shows that this phenomenon correlates with a haemodynamic network involving the insula, the cingulate and the basal forebrain. The constellation of these areas may act as a pacemaker of the CAP manifestation, as a result of the regulation of the vigilance level during sleep.

Introduction

The EEG of NREM sleep in humans is characterized by pseudo-periodic phasic events referred to as the cyclic alternating pattern (CAP)[1, 2]. Two phases, consisting of a variety of sleep EEG waves and rhythms, alternate throughout NREM: a synchronization phase A (CAP-A), appearing as runs of regular or irregular high voltage EEG delta, with or without higher frequency components, standing out of the EEG background; and a de-synchronization phase B (CAP-B), appearing as lower-voltage EEG constituting the background of NREM[3-5] (Figure 1). Although CAPs were first observed in comatose patients[1], where A-phases were found to be strongly related to increased muscle activity, heart rate and restlessness, and positively correlated to the clinical outcome[6], it soon became apparent that CAPs are an essential part of normal sleep[2, 7, 8]. CAPs can be elicited by somatosensory stimulation[1], and auditory perturbation[9]. Being a robust NREM microstructural element, the CAP has distinctive properties: a) the majority of sleep stage transitions are mediated by CAP sequences[2], b) CAP density and patterns vary both amongst sleep cycles[10] and sleep stages[11], being more frequent in the first sleep cycles, and c) CAP patterns vary between the descending and ascending branches of NREM[12, 13], occurring predominantly during the descending NREM phases of each sleep cycle.

The CAP has been proposed as a gating mechanism supporting the continuation of sleep after its initiation and into the deeper stages of NREM. The rate of CAP-A/CAP-B cycling in NREM sleep decreases exponentially after sleep onset in parallel with the homeostatic decay of slow wave activity responding to sleep pressure according to the Borbély's S process[14], predominating the descending branch of NREM of the first sleep cycles and increasing when environmental noise increases[5, 15]. It is therefore surmised that the input-dependent CAP-A events are hypnagogic, contributing to the build-up of slow wave sleep, and following the course of the homeostatic process, which is considered to depend on cortical metabolism[16].

During states of reduced vigilance, the CAP appears to have a fundamental role in supporting sleep

maintenance by complementing sleep bi-stability[17] with lability and reversibility[16]. The later provides flexible adaptation to environmental stimuli for the system to shield itself from sensorial inputs. Consistent with the view of NREM sleep being an emergent property of loosely coupled local processes[18-20], it has been proposed that the homeostatic pressure for sleep may be reflected locally as EEG slowing. The processes providing the infra-slow oscillation (0.01–0.1 Hz) have been proposed to reflect neural correlates of large-scale fluctuations, related to neuronal excitability and arousal, appearing on the EEG as phases of the CAP[16, 21]. Both metabolic and electrophysiological studies show that the human NREM sleep is an active state largely driven by homeostatic sleep pressure and infra-slow oscillations linked to that pressure. During the latter, brain activity is temporally organized by spontaneous EEG rhythms in a regionally specific manner[19, 20, 22, 23]. This relation of the temporal organization of brain activity to local homeostasis confers importance to the investigation of the metabolic correlates of the CAP in different brain areas.

The neural correlates of the CAP have been investigated only recently, yet without convergence. EEG spectrum-based source imaging has related the CAP to a distribution of frontal, midline and occipito-parietal sources[24]. Near-infrared spectroscopy on the forehead and systemic haemodynamics have related the CAP to changes in global scalp, cortical, and systemic hemodynamic signals that resemble the ones seen in arousal[25]. EEG-fMRI is a well-documented non-invasive neuroimaging technique that allows haemodynamic fluctuations associated with EEG phenomena to be mapped throughout the brain volume[26-29]. By identifying blood oxygen-level dependent (BOLD) changes related to A phases of the CAP, using EEG-fMRI, this study aims in determining the brain regions haemodynamically associated with the CAP-A synchronization phase during NREM sleep.

Methods

Participants

Twenty-nine (29) subjects from a pool of 66 patients who had EEG-fMRI assessment for their epilepsy at St. Luke's Hospital, Thessaloniki, Greece during the period 2010-2016, were selected for this study. Inclusion criteria were: 1) spontaneous achievement of more than 20 minutes of continuous uninterrupted NREM sleep of depth no less than stage II, 2) lack of epileptic seizures during the EEG-fMRI scan, and 3) MRI negative patients, or patients with topographically limited solitary lesions, including cortical dysplasia, polymicrogyria, hippocampal sclerosis, and chronic post-traumatic cortical changes, thereby ensuring that our study is free of effects owing to major structural cerebral anomalies that could affect the results. No sleep-promoting medication was administered to the selected subjects. Twenty-two (22) of the selected subjects were partially sleep-deprived the previous night (having had 3-4 hours of sleep) and had been awake for at least 10 hours prior to the recording as an attempt to increase their epileptic activity during the interictal EEG-fMRI study; seven (7) subjects slept spontaneously without prior sleep deprivation; thirteen (13) females; mean subject age: 22 years (range: 11-45) (Supplementary Table 1).

All subjects provided informed consent according to the Declaration of Helsinki. All procedures were approved by St. Luke's Ethics Committee.

EEG-fMRI acquisition parameters. Functional imaging consisted of gradient-echo T2*-weighted single-shot echo-planar (EPI) images (45 2.5mm slices of 0.3mm inter-slice distance, TE/TR: 45/4000msec, 90^{o} flip angle, FOV 240cm^{2}, 96x96 matrix, iPAT), acquired by a 1.5T Avanto MR scanner (Siemens AG, Germany). A 32-channel MR-compatible electrode cap (BrainCap MR, Easycap, Herrsching-Breitbrunn, Germany) was used for EEG, signals were amplified by x1500, band-pass filtered at 0.016Hz-1kHz, digitized at 16-bit and sampled at 5kHz by a MR-compatible BrainAmp system (BrainAmp MR plus, Brain Products, Munich, Germany).

An additional derivation was used to record the electrocardiogram (ECG) and all electrode impedances were kept below 10kOhm throughout the recording in the MR scanner. All neurophysiological data were recorded on workstations located outside the MR scanner room through fiber-optic cables, synchronized with the MR scanner clock and a scanner-derived trigger signal initiating each EPI volume acquired. EEG-fMRI sessions were either 30 or 60 minutes long.

EEG processing. The EEG gradient- and cardiac-related artifacts were removed off-line by application of averaged artifact template subtraction methods embedded in the BrainVision Analyzer 2.0 software (Brain Products, Munich, Germany)[30]. The sleep EEG was scored based on the standard AASM criteria[31], using a 1-70 Hz display filter. CAPs were determined visually based on the criteria set forth by the Parma group[32]. The A phases of CAP were identified and marked as blocks of mixed patterns of high-voltage waves and rhythms (including, but not exclusively, vertex waves, K-complexes, spindles, delta waves, theta and alpha runs), occurring during NREM sleep, contrasted to the background low-voltage EEG (B phase of CAP). NREM sleep stages were scored, with NREM I being the lightest stage and slow wave sleep (SWS) being the deepest. A CAP sequence was determined by the succession of at least 2 CAP cycles (a pair of A-B phases makes a CAP cycle). The minimal duration of a CAP-A or B phase was set to 2 sec and the maximum was 60 sec; absence of CAP sequence for more than 60 sec was scored as non-CAP (NCAP). In this study we did not account for the different CAP-A subtypes, but rather treated CAP-A phases as a single EEG phenomenon. However, A-phases characterized by increased somatomotor activity, accompanied by profound muscle artifact, and alpha-band EEG content were not included in the study. Marking of ambiguous onsets and offsets of CAP-A blocks was facilitated in a case by case manner by butterfly plots (Figure 1b), as well as time-frequency analysis, the latter combining Morlet wavelet transform (power measurements, linear frequency range: 1-70 Hz, step: 0.5 Hz, central frequency: 1 Hz, time resolution 3 sec, with 1/f compensation for spectral

flattening), enhancing the high-frequency content of the signal, and multitaper fast fourier transform (FFT; Hanning taper, range: 1-70 Hz, step: 0.5 Hz, modulation factor: 10, time resolution: 200 msec, time step: 50 msec), enhancing the low frequency content of the EEG (Figure 1c).

fMRI processing. The first 2 EPI volumes of the fMRI series were discarded from further analysis to allow for T1 saturation. In accordance with standard fMRI processing practice, the rest of the images were spatially realigned, normalized in MNI space, and spatially smoothed with a cubic Gaussian kernel of 8 mm full width at half maximum. A General Linear Model (GLM) was built using SPM12 (www.fil.ion.ucl.ac.uk/SPM12). CAP-A phases were included in the GLM as the main regressor and modeled as blocks of variable duration that were convolved with the canonical Haemodynamic Response Function (HRF). Since CAP-A phases exhibit variable durations from 2 to 60 sec[3], a temporal filter of 128 TR was used to account for signal changes of up to 2 minutes. CAP-B phases served as baseline. Five sets of confound regressors were added to the GLM: a) the periods of relaxed wakefulness, that is, the onset of the recording where our subjects were relaxed and their EEG was characterized by abundance of the posterior alpha rhythm (modelled as blocks of variable duration); b) the Non-CAP periods, according to the scoring criteria described in the previous subsection (modelled as blocks of variable duration); c) the interictal epileptic discharges, that is, the individual paroxysmal epileptic EEG elements in the form of spike-waves, sharp waves or polyspike activity (modelled as short transients when occurring in isolation, or blocks of variable duration when occurring either in clusters or as persistent epileptic discharges); d) a set of cardiac confound regressors was included in the GLM to account for periodic pulse-related BOLD changes, as determined by the ECG R-wave[33]; e) motion-related effects, determined by 3 displacement (x, y, z, in mm) and 3 rotational (pitch, roll, yaw, in degrees) metrics of the head after spatial re-alignment of the images, were also included in the GLM as 24 regressors of the 6 realignment parameters Volterra expansion[34], plus Heaviside step function

combinations to account for large motion effects ("scan nulling" regressors with 0.2 mm threshold)[35]. The null hypothesis of the GLM is that there is no cluster of voxels BOLD-correlated to the EEG manifestations of sleep instability. At the level of individual subjects, maps of t-plus contrast for the effect of CAP-A were obtained with a significance threshold of $p<0.001$. We then sought to identify typical effects using a random effects model based on the contrast maps generated at the individual subject level. We used multiple regression with 3 covariate vectors accounting for the group variability in age, gender and state during the scan (partially sleep-deprived or not) to remove systematic interference from BOLD signal changes owing to putative individual syndrome-related epileptic activity and presented results both uncorrected ($p < 0.001$) and family-wise error (FWE) corrected for multiple comparisons ($p < 0.05$) based on random field theory[36]. Subjects were further separated into groups in terms of age (3 groups: 10-19, 20-29, and more than 30 years old groups), gender (2 groups), and partial sleep deprivation (2 groups: partial sleep and non-sleep deprived groups). One-sample t-test uncorrected ($p < 0.001$) ANOVA was used for all derived groups. Conjunction analysis was in turn used between groups of each category to assess the consistency of random effects analysis clusters against outliers that may bias group-level statistics[37].

Results

Thirty subjects underwent a total of 1,450 minutes of EEG-fMRI scanning and achieved a total of 1,058 minutes of NREM sleep, within which a total of 2,388 CAP-A phases were identified and in turn contrasted against the CAP-B desynchronization phases at the individual subject level (Supplementary Figure 1, Supplementary Table 1).

We found positive BOLD changes correlated to the CAP-A phase in the following regions with bilateral distribution: the insula (Brodmann area 14/15; Left: x=-36, y=0, z=6, $p_{FWE\text{-}corr} < 0.0001$, $q_{FDR\text{-}corr} < 0.0001$, $T = 9.55$, $Z = 6.14$, $p_{uncorr} < 0.0001$; Right: x=44, y=0, z=4, $p_{FWE\text{-}corr} < 0.0001$, $q_{FDR\text{-}corr} <$

0.0001, T = 11.88, Z = 6.82, $p_{uncorr} < 0.0001$), the middle cingulate gyrus (Brodmann area 24; x=-4, y=2, z=40, $p_{FWE-corr} < 0.0001$, $q_{FDR-corr} < 0.0001$, T = 9.34, Z = 6.07, $p_{uncorr} < 0.0001$), and the basal forebrain (Brodmann area 25; Left: x=-20, y=2, z=-12,$p_{FWE-corr} < 0.0001$, $q_{FDR-corr} = 0.007$, T = 9.03, Z = 5.97, $p_{uncorr} < 0.0001$; Right: x=16, y=-2, z=-6, $p_{FWE-corr} < 0.0001$, $q_{FDR-corr} = 0.013$, T = 8.62, Z = 5.82, $p_{uncorr} < 0.0001$) (Figure 2). No suprathreshold values were derived for each of the 3 covariates (age, gender, state) of multiple regression, for both negative and positive correlation to the main variable. Group level one-way ANOVA and conjunction analysis confirmed the spatial pattern of the CAP-A BOLD correlates in all age and gender groups (Supplementary Figure 2, 3), as well as in subjects who were partially sleep-deprived prior to the scan (Supplementary Figure 4).

Discussion

In this sleep EEG-fMRI study, we selected recordings from 30 subjects in whom long periods of NREM sleep were captured during functional MRI scanning. We identified NREM periods of CAP sequences and marked the A-phases characterized by EEG synchronization. The group analysis revealed prominent CAP-A related BOLD changes in the insula, the middle cingulate gyrus and the basal forebrain. The hereby revealed consistency of BOLD changes strongly associated with the CAP-A phases support the authenticity of the CAP as an EEG phenomenon of NREM sleep. In addition, our results retrospectively validate the EEG scoring criteria for CAP definition as initially set by the Parma group[3, 32].

The insular involvement stands out as a prominent feature of CAP-A related BOLD signal changes in this study, along with concordant changes of the cingulate cortex and the basal frontal region. This pattern is consistent with anatomical tracing studies in primates[38] confirming dense insular interconnections with the cingulate cortex[39, 40] and limbic areas[41, 42]. The insula is a known node of sensory and autonomic information processing. Acute intraoperative cortical electrical stimulation has

multiple times verified its wide functional diversity, as it can produce motor, somatosensory (including generalized sensations of warmth and cold) and auditory responses, pain, speech and oropharyngeal disturbances, as well as autonomic-vegetative responses such as hypogastric sensations, respiratory acceleration, anxiety attacks, and rotation/tension sensation[43-47]. However, most interesting is the role of the insula as a key structure for switching between the resting and the alert brain states[48-50], as well as mediating focal attention[51]. The central role of the insula underlying CAP-A phases is consistent with its function as a node of converging multimodal, exteroceptive and interoceptive stimuli, complemented by its relationship to behavioral alertness and attention.

The implication of the cingulate gyrus in sleep is no surprise, as literature has already revealed the contribution of the posterior cingulate in the generation of SWS[52], the contribution of the middle cingulate in the generation of the spontaneous K-complex of NREM sleep stage II[53, 54] and vertex waves[55], as well as that of the anterior cingulate for fast and slow sleep spindles generation[56], and for all lower-frequency bands in MEG studies[57]. As the EEG expression of the CAP-A phases comprise an irregular constellation of the above rhythms and waves, the BOLD-correlated signal changes over the cingulate cortex could be attributed to their generation. However, there is an alternative/complementary explanation stemming from the fact that in the alert brain states, the cingulate has been highly correlated to the initiation of voluntary complex motor behavior[58]; the middle cingulate specifically for spontaneous action intention[59] and pre-movement activity for voluntary actions[60]. More importantly, the activation of the middle cingulate has been reliably shown to precede sleepwalking episodes[61] and NREM parasomnia arousals[62, 63]. This evidence, combined with the hypothesis that the CAP is an EEG expression of the level of vigilance during human sleep, could set a key role for the middle cingulate in the primary CAP-A network as an anticipatory/preparatory region for motor reactivity and responsiveness.

Of particular interest is the involvement of the basal frontal region, that has been identified as an important structure in the sleep-wake control[64-66], functionally interacting with pontine nuclei to regulate breathing[67], regulating vigilance through a balanced mechanism between cholinergic and GABAergic projections to the cortex[68, 69]. In addition, the basal forebrain has been reliably shown by fMRI to have high correlation of response to visceral stimuli, such as heart rate and blood pressure alterations[70], features known to accompany CAP-A phases during sleep[5, 71]. However, most interesting in the context of our findings is the cognitive role of the basal forebrain in decision-making and error monitoring procedures, integrated through coordinated anterior insular interactions[72-74]. As shown, the insula conveys error-related signals to the basal forebrain in order to promote learning and adaptive behavior[75]. In the context of CAP being a manifestation of the vigilance level during sleep, the basal forebrain could be mediating adaptive procedures to the sleeping environment.

Previous attempts to delineate the neural correlates of the CAP through other modalities have been few and did not converge to a robust network. Source imaging based on EEG time-frequency analysis of the CAP resulted in anterior frontal and midline sources for the low-frequency EEG constituents of the CAP and posterior occipito-parietal sources for the higher frequencies[24]. The use of localized near-infrared spectroscopy (NIRS) showed diffuse cortical, and systemic hemodynamic signals related to the CAP under the probe, resembling arousal patterns [25]. Although both techniques are limited by their low spatial resolution, the diffuse character of cortical activations encountered in our EEG-fMRI single-subject analysis (Supplementary Figure 1) is concordant with the results of both studies. The high spatial resolution of the EEG-fMRI allowed us to reveal a cluster of cortical regions strongly correlated to the A phases of the CAP, whose activity is unlikely to be picked up by either the EEG or NIRS.

The fact that all participants suffered from epilepsy, given the known co-existence of interictal discharges with CAP-A phases, constitutes a limitation in this study. However, potential biases were treated at both the individual and group levels. At the single-subject level, each individual GLM

included interictal epileptiform activity of scalp EEG as a regressor in order to account for the respective effects. Final results were validated only from random effects and conjunction analysis that, given the variable distribution of our subject's pathologies (Supplementary Table 1), we expect have confidently eliminated effects owing to potential syndrome-related false-positive correlations. Another limitation this project faced is the technical inability to study the different CAP subtypes[5], due to the increased somatomotor activity that accompanies one of them (CAP-A3) and severely distorts the echo-planar images acquired. Given the fact that CAP-A1 and CAP-A2 subtypes are fairly similar in terms of both including high-amplitude low-frequency hypersynchronous EEG elements, combined with the fact they are both expressions of the vigilance level during sleep, we decided to focus this work on the correlates of the CAP as a sequence alone without suggesting that the two subtypes are one and the same phenomenon.

Our findings lead us to hypothesize that the CAP-A correlated haemodynamic network acts as a synchronization pacemaker, orchestrating the reactive EEG grapho-elements into synchrony in order to control the level of NREM sleep vigilance and the sleeper's arousability. The constituents of this brain network can mediate arousing stimuli that have the potential to initiate the CAP sequence, produce its distinctive EEG pattern, and manifest its somatomotor and autonomic correlates, as well as account for the enhanced reactivity of CAP-A phases to subliminal stimulation[5]. The insula, as a multimodal stimuli processing and state-switching node, can either maintain sleep continuity or switch to a higher level of vigilance depending on the nature of the perturbation. The cingulate at the same time can be involved in preparing potential motor components of the reaction to the arousing stimulus that tends to de-stabilize sleep. The basal forebrain can in turn monitor the insular behavior and mediate efficient adaptation to the environmental perturbations. In addition, the hereby revealed consistency of BOLD changes-derived spatial pattern strongly associated with the CAP-A phases retrospectively validate the EEG scoring criteria for CAP definition as initially set by the Parma group[32] and further support the authenticity of

the CAP as an EEG phenomenon of NREM sleep.

Acknowledgements

We thank Dr. Petia Dimova of St. Naum University Hospital in Sofia, Bulgaria, and Dr. Dimitrios Kazis of Papanikolaou General Hospital of Thessaloniki, Greece for referring patients.

Funding

This study was partially funded by the European Commission under the 7th Framework Programme (project number 287720). Dr. Serge Vulliémoz was supported by Swiss National Science Foundation grants 141165 and 140332.

Note

Conflict of interest statement. The authors have no conflict of interest to disclose.

References

1. Terzano MG, et al. The cyclic alternating pattern as a physiologic component of normal NREM sleep. *Sleep*. 1985;**8**:137-145.
2. Terzano MG, et al. The cyclic alternating pattern sequences in the dynamic organization of sleep. *Electroencephalogr Clin Neurophysiol*. 1988;**69**:437-447.
3. Terzano MG, et al. Atlas, rules and recording techniques for the scoring of cyclic alternating pattern (CAP) in human sleep. *Sleep Med*. 2002;**2**:537-553.
4. Iber C, et al. *The AASM manual for the scoring of sleep and associated events: rules, terminology and technical specifications*. 1st ed. Westchester, IL: American Academy of Sleep Medicine; 2007.
5. Parrino L, et al. Cyclic alternating pattern (CAP): The marker of sleep instability. *Sleep Med Rev*. 2012;**16**:27-45.
6. Valente M, et al. Sleep organization pattern as a prognostic marker at the subacute stage of post-traumatic coma. *Clin Neurophysiol*. 2002;**113**:1798-1805.
7. Steriade M, et al. Cortical and thalamic cellular correlates of electroencephalographic burst-suppression. *Electroencephalogr Clin Neurophysiol*. 1994;**90**:1-16.
8. Parrino L, et al. CAP, epilepsy and motor events during sleep: the unifying role of arousal. *Sleep Med Rev*. 2006;**10**:267-285.
9. Terzano MG, et al. Modifications of sleep structure induced by increasing levels of acoustic perturbation in normal subjects. *Electroencephalogr Clin Neurophysiol*. 1990;**76**:29-38.
10. Terzano MG, et al. CAP components and EEG synchronization in the first 3 sleep cycles. *Clin Neurophysiol*. 2000;**111**:283-290.
11. Terzano MG, et al. CAP and arousals are involved in the homeostatic and ultradian sleep process. *J Sleep Res*. 2005;**14**:359-368.

12. Ferrillo F, et al. Comparison between visual scoring of cyclic alternating pattern (CAP) and computerized assessment of slow EEG oscillations in the transition from light to deep non-REM sleep. *J Clin Neurophysiol*. 1997;**14**:210-216.

13. Halász P, et al. The nature of arousal in sleep. *J Sleep Res*. 2004;**13**:1-23.

14. Borbély AA. A two process model of sleep regulation. *Hum Neurobiol*. 1982;**1**:195–204.

15. Halász P. K-complex, a reactive EEG graphoelement of NREM sleep: an old chap in a new garment. *Sleep Med Rev*. 2005;**9**:391-412.

16. Halász P, Bódizs R. *Dynamic structure of NREM sleep*. London: Springer-Verlag; 2013.

17. Saper CB, et al. Sleep state switching. *Neuron*. 2010;**68**:1023-1042.

18. Krueger JM, et al. Sleep as a fundamental property of neuronal assemblies. *Nat Rev Neurosci*. 2008;**9**:910-919.

19. Nir Y, et al. Regional slow waves and spindles in human sleep. *Neuron*. 2011;**70**:153–169.

20. Nobili L, et al. Local aspects of sleep: observations from intracerebral recordings in humans. *Prog Brain Res*. 2012;**199**:219-232.

21. Lörincz ML, et al. ATP-dependent infra-slow (<0.1 Hz) oscillations in thalamic networks. *PLoS One*. 2009;**4**:e4447.

22. Mascetti L, et al. Spontaneous neural activity during human non-rapid eye movement sleep. *Prog Brain Res*. 2011;**193**:111-118.

23. Ioannides AA, et al. MEG identifies dorsal medial brain activations during sleep. *Neuroimage*. 2009;**44**:455-68.

24. Ferri R, et al. Topographic mapping of the spectral components of the cyclic alternating pattern (CAP). *Sleep Med.* 2005;**6**(1):29-36.

25. Näsi T, et al. Cyclic alternating pattern is associated with cerebral hemodynamic variation: a near-infrared spectroscopy study of sleep in healthy humans. *PLoS One* 2012;**7**:e46899.

26. Ives JR, et al. Monitoring the patient's EEG during echo planar MRI. *Electroencephalogr Clin Neurophysiol*. 1993;**87**:417-420.

27. Warach S, et al. EEG-triggered echo-planar functional MRI in epilepsy. *Neurology*. 1996;**47**:89-93.

28. Lemieux L, et al. Event-related fMRI with simultaneous and continuous EEG: description of the method and initial case report. *Neuroimage*. 2001;**14**:780-787.

29. Laufs H. A personalized history of EEG-fMRI integration. *Neuroimage*. 2012;**62**:1056-1067.

30. Allen PJ, et al. A method for removing imaging artifact from continuous EEG recorded during functional MRI. *Neuroimage*. 2000;**12**:230–239.

31. American Academy of Sleep Medicine (AASM). The visual scoring of sleep in adults. *J Clin Sleep Med.* 2007;**3**:121-135.

32. Terzano MG, Parrino L. Functional relationship between micro- and macrostructure of sleep. In: Terzano MG, et al. ed. *Phasic events and dynamic organization of sleep*. New York: Raven Press; 1991: 101-119.

33. Liston AD, et al. Modelling cardiac signal as a confound in EEG–fMRI and its application in focal epilepsy studies. *Neuroimage.* 2006;**30**:827–834.

34. Friston KJ, et al. Movement-related effects in fMRI time-series. *Magn Reson Med*. 1996;**35**:346–355.

35. Lemieux L, et al. Modelling large motion events in fMRI studies of patients with epilepsy. *Magn Reson Imaging*. 2007;**25**:894–901.

36. Friston KJ, et al. Comparing functional (PET) images: the assessment of significant change. *J Cereb Blood Flow Metab*. 1991;**11**:690-699.

37. Friston KJ, et al. Multisubject fMRI studies and conjunction analyses. *NeuroImage*. 1999;**10**:385-369.

38. Augustine JR. Circuitry and functional aspects of the insular lobe in primates including humans. *Brain Res Rev*. 1996;**22**:229-244.

39. Vogt BA, et al. Cingulate cortex of the rhesus monkey I. Cytoarchitecture and thalamic afferents. *J Comp Neurol*. 1987;**262**:256-270.

40. Vogt BA, Pandya DN. Cingulate cortex of the rhesus monkey II. Cortical afferents. *J Comp Neur*. 1987;**262**:271-289.

41. Mufson EJ, et al. Insular interconnections with the amygdala in the rhesus monkey. *Neuroscience*. 1981;**6**:1231-1248.

42. Augustine JR. The insular lobe in primates including humans. *Neurol Res*. 1985;**7**:2-10.

43. Penfield W, Jasper H. *Epilepsy and the functional anatomy of the human brain*. Boston, MA: Little Brown; 1954.

44. Penfield W, Faulk ME. The insula; further observations on its function. *Brain*. 1955;**78**:445–470.

45. Penfield W, Rassmussen T. *The cerebral cortex of man: a clinical study of localization*. New York: Macmillan; 1957.

46. Lüders H, et al. The second sensory area in humans: evoked potentials and electrical stimulation studies. *Ann Neurol*. 1985;**17**:177-184.

47. Afif A, et al. Anatomofunctional organization of the insular cortex: A study using intracerebral electrical stimulation in epileptic patients. Epilepsia. 2010;**51**:2305-2315.

48. Seeley WW, et al. Dissociable intrinsic connectivity networks for salience processing and executive control. *J Neurosci*. 2007;**27**:2349-2356.

49. Sridharan D, et al. A critical role for the right fronto-insular cortex in switching between central-executive and default-mode networks. *Proc Natl Acad Sci USA*. 2008;105:12569-12574.

50. Tang YY, et al. Neural correlates of establishing, maintaining, and switching brain states. *Trends Cogn Sci*. 2012;**16**:330-337.

51. Nelson SM, et al. Role of the anterior insula in task-level control and focal attention. *Brain Struct Funct*. 2010;**214**:669-680.

52. Dang-Vu TT, et al. Spontaneous neural activity during human slow wave sleep. *Proc Natl Acad Sci USA*. 2008;**105**:15160-15165.

53. Jahnke K, et al. To wake or not to wake? The two-sided nature of the human K-complex. *Neuroimage*. 2012;**59**:1631–1638.

54. Caporro M, et al. Functional MRI of sleep spindles and K-complexes. *Clin Neurophysiol*. 2012;**123**:303-309.

55. Stern JM, et al. Functional imaging of sleep vertex sharp waves. *Clin Neurophysiol*. 2011;**122**:1382-1386.

56. Schabus M, et al. Hemodynamic cerebral correlates of sleep spindles during human non-rapid eye movement sleep. *Proc Natl Acad Sci USA*. 2007;**104**:13164–13169.

57. Ioannides AA, et al. Using MEG to understand the progression of light sleep and the emergence and functional roles of spindles and K-complexes. *Front Hum Neurosci*. 2017;**11**:313.

58. Talairach J, et al. The cingulate gyrus and human behavior. *Electroencephalogr Clin Neurophysiol*. 1973;**34**(1):45-52.

59. Hoffstaedter F, et al. The ‘‘what’’ and ‘‘when’’ of self-initiated movements. *Cereb Cortex*. 2013;**23**:520–530.

60. Nguyen VT, et al. Reciprocal interactions of the SMA and cingulate cortex sustain premovement activity for voluntary actions. *J Neurosci*. 2014;**34**:16397–16407.

61. Januszko P, et al. Sleepwalking episodes are preceded by arousal-related activation of the cingulate motor area: EEG current density imaging. *Clin Neurophysiol*. 2016;**127**:530-536.

62. Terzaghi M, et al. Evidence of dissociated arousal states during NREM parasomnia from an intracerebral neurophysiological study. *Sleep*. 2009;**32**:409–12.

63. Terzaghi M, et al. Dissociated local arousal states underlying essential clinical features of non-rapid eye movement arousal parasomnia: an intracerebral stereoelectroencephalographic study. *J*

Sleep Res. 2012;**21**:502–506.

64. Szymusiak R. Magnocellular nuclei of the basal forebrain: substrates of sleep and arousal regulation. *Sleep*. 1995;**18**:478–500.
65. Semba K. Multiple output pathways of the basal forebrain: organization, chemical heterogeneity, and roles in vigilance. *Behav Brain Res*. 2000;**115**:117–141.
66. Stenberg D. Neuroanatomy and neurochemistry of sleep. *Cell Mol Life Sci*. 2007;**64**:1187–1204.
67. Douglas CL, et al. Pontine and basal forebrain cholinergic interaction: implications for sleep and breathing. *Respir Physiol Neurobiol*. 2004;**143**:251-262.
68. Lelkes Z, et al. Cholinergic basal forebrain structures are involved in the mediation of the arousal effect of noradrenaline. *J Sleep Res*. 2013;**22**:721-726.
69. Xu M, et al. Basal forebrain circuit for sleep-wake control. *Nat Neurosci*. 2015;**18**(11):1641-1647.
70. King AB, et al. Human forebrain activation by visceral stimuli. *J Comp Neurol*. 1999;**413**:572-582.
71. Terzano MG, Parrino L. Origin and significance of cyclic alternating pattern (CAP). *Sleep Med Rev*. 2000;**4**:101-123.
72. Ullsperger M, von Cramon DY. Subprocesses of performance monitoring: a dissociation of error processing and response competition revealed by event-related fMRI and ERPs. *Neuroimage*. 2001;**14**:1387–1401.
73. Wessel JR, et al. Surprise and error: common neuronal architecture for the processing of errors and novelty. *J Neurosci*. 2012;**32**:7528–7537.
74. Vinckier F, et al. Neuro-computational account of how mood fluctuations arise and affect decision making. *Nat Commun*. 2018;**9**(1):1708.
75. Bastin J, et al. Direct recordings from human anterior insula reveal its leading role within error-monitoring network. *Cereb Cortex*. 2017;**27**:1545-1557.

Figure Legends

Figure 1. The NREM cyclic alternating pattern (CAP). (a) Sleep EEG with two phases of synchronization standing out of the NREM background. (b) Butterfly plot of all EEG electrodes for the same period, overlaid with cumulative spectral power charts for each scored CAP-A and CAP-B phase. (c) Wavelet and FFT-based time-frequency plots derived from F4 electrode showing the contrast between phases of synchronization (CAP-A) and de-synchronization (CAP-B) in the frequency domain.

Figure 2. The BOLD correlates of the NREM CAP. (a-d) Glass brain and T1-overlaid uncorrected and corrected contrast maps of group-level analysis corresponding to the CAP-A variable (T subscript denotes degrees of freedom). The design matrix of the multiple regression model for the CAP-A variable (1) is presented, with three regressors for age (2), gender (3) and state (4); the latter referring to the subject been scanned partially sleep deprived or not. Both uncorrected and corrected contrast maps revealed statistically significant changes in BOLD signal bilateral over the insulas (Brodmann area 14/15), the middle cingulate gyrus (Brodmann area 24) and the basal forebrain (Brodmann area 25). (e) 3D surface projection of the corrected contrast clusters.

Abbreviations

EEG: Electroencephalography / Electroencephalogram

fMRI: Functional magnetic resonance imaging

MRI: Magnetic resonance imaging

CAP: Cyclic alternating pattern

NREM: Non-rapid eye movement

BOLD: blood oxygen-level dependent

EPI: Echo-planar imaging

GLM: General linear model

HRF: Haemodynamic Response Function

FWE: Family-wise error

FDR: False discovery rate

SUPPLEMENTARY MATERIAL

Supplementary Figure Legends

Supplementary Figure 1. Fixed effects analysis CAP-A correlates. Glass brain-overlaid, fixed effects analysis-derived, uncorrected contrast maps of CAP-A synchronization phases from each of the 30 subjects (T subscript denotes degrees of freedom). Notice the high variability of BOLD signal across subjects, that makes the derivation of a common pattern difficult.

Supplementary Figure 2: Random effects and conjunction analysis across age groups. (a,b) BOLD correlates of the CAP-A synchronization phase for 15 subjects between ages of 10 and 19 years old, projected on glass brain and overlaid on a normalized T1 brain. (c,d) BOLD correlates of the CAP-A synchronization phase for 7 subjects between ages of 20 and 29 years old. (e,f) BOLD correlates of the CAP-A synchronization phase for 8 subjects more than 30 years old. Statistical power can vary between age groups as a result of the different number of participants in each group. (g,h) Conjunction across all 3 age groups.

Supplementary Figure 3. Random effects and conjunction analysis across gender groups. (a,b) BOLD correlates of the CAP-A synchronization phase for 16 male subjects, projected on glass brain and overlaid on a normalized T1 brain. (c,d) BOLD correlates of the CAP-A synchronization phase for 14 female subjects. (e,f) Conjunction across the 2 groups.

Supplementary Figure 4. Random effects and conjunction analysis across partially sleep-deprived and non sleep-deprived groups. (a,b) BOLD correlates of the CAP-A synchronization phase for 22 partially sleep-deprived subjects, projected on glass brain and overlaid on a normalized T1 brain. (c,d) BOLD

correlates of the CAP-A synchronization phase for 8 non sleep-deprived subjects. Statistical power can vary between these groups as a result of the different number of participants in each group. (e,f) Conjunction across the 2 groups.

TABLES

Supplementary Table 1. Demographic, pathology/treatment and EEG-fMRI recording data of the selected participants (L: left, R: right, B: bilateral, FLE: frontal lobe epilepsy, PLE: parietal lobe epilepsy, TLE: temporal lobe epilepsy, ILE: insular lobe epilepsy, OLE: occipital lobe epilepsy, JAE: juvenile absence epilepsy, JME: juvenile myoclonic epilepsy, IGE: idiopathic generalized epilepsy, CBZ: carbamazepine, CLM: clobazam, LCM: lacosamide, LEV: levetiracetam, LTG: lamotrigine, OXC: oxcarbazepine, PB: phenobarbital, RUF: rufinamide, TPM: topiramate, VPA: valproic acid, ZNS: zonisamide, *: spontaneous sleep after partial deprivation, SWS: slow wave sleep).

Subjects	Age	Sex	Diagnosis	Anti-epileptic medication	Seizure frequency	Scan time (min)	Total NREM sleep time (min)	NREM Sleep stages	CAP-As
1	12	M	PLE (B)	LEV, OXC, VPA	2-3/day	30	27	I, II, SWS	31
2	30	M	JME	VPA	3-4/year	60	23	I, II	41
3	11	M	OLE (L)	LEV, LTG, OXC, VPA	5-10/day	30	23*	I, II	45
4	14	F	OLE (R)	LCM, LEV, VPA	2-3/week	60	51*	I, II	128
5	24	M	TLE (R)	LEV, OXC,	5-10/month	60	48	I, II, SWS	107

				VPA					
6	11	M	FLE (R)	LEV, VPA	1-3/day	60	33*	I, II, SWS	111
7	16	F	TLE (R)	CBZ, TPM	1-2/week	30	27*	I, II, SWS	45
8	16	M	FLE (L)	CBZ, LEV	3-4/year	60	43*	I, II	56
9	25	F	PLE (B)	CBZ, LEV, VPA, ZNS	15-20/day	60	56*	I, II, SWS	69
10	31	M	TLE (R)	LEV, OXC	1-2/month	60	21	I, II	52
11	11	F	OLE (L)	LEV, RUF	3-5/month	30	24*	I, II, SWS	60
12	38	F	TLE (R)	OXC, TPM	4-10/year	60	53	I, II, SWS	71
13	15	F	FLE (R)	CLM, VPA	10-30/day	60	51*	I, II, SWS	153
14	19	F	TLE (L)	CLM, LEV, OXC	8-20/month	30	26	I, II	57
15	19	M	PLE (R)	LEV, OXC	1-4/day	30	25*	I, II, SWS	49
16	18	F	TLE (R)	LEV, OXC, LCM	2-4/week	60	49*	I, II, SWS	150
17	27	F	FLE (L)	CLM, LCM, TPM, VPA	1-4/week	30	25	I, II, SWS	53

18	35	M	FLE (L)	CBZ, OXC	2-3/week	30	27*	I, II, SWS	50
19	30	M	FLE (R)	CBZ, OXC, ZNS	1-5/week	30	24*	I, II	40
20	20	M	TLE (L)	LEV, OXC	1-4/month	60	49*	I, II, SWS	111
21	17	F	FLE (L)	CBZ, LTG	1-2/month	60	54*	I, II, SWS	218
22	19	M	FLE (L)	LEV, OXC, VPA	3-7/week	60	48*	I, II, SWS	98
23	13	M	IGE	LEV, TPM, VPA	10-30/day	60	51*	I, II, SWS	131
24	42	F	TLE (R)	LEV, OXC	1-2/week	60	42*	I, II, SWS	71
25	13	F	ILE (L)	CBZ, OXC	1-2/month	60	28*	I, II	66
26	27	F	TLE (R)	LEV, OXC, LCM	1-3/week	60	25*	I, II	56
27	35	M	ILE (L)	CLB, LTG, OXC, VPA	10-20/month	60	55*	I, II, SWS	97
28	27	M	FLE (R)	VPA	1/month	60	22*	I, II	38
29	45	M	FLE (R)	OXC, PB	1-6/month	40	28*	I, II, SWS	134

	Total: 1,450	Total: 1,058	Total: 2,388

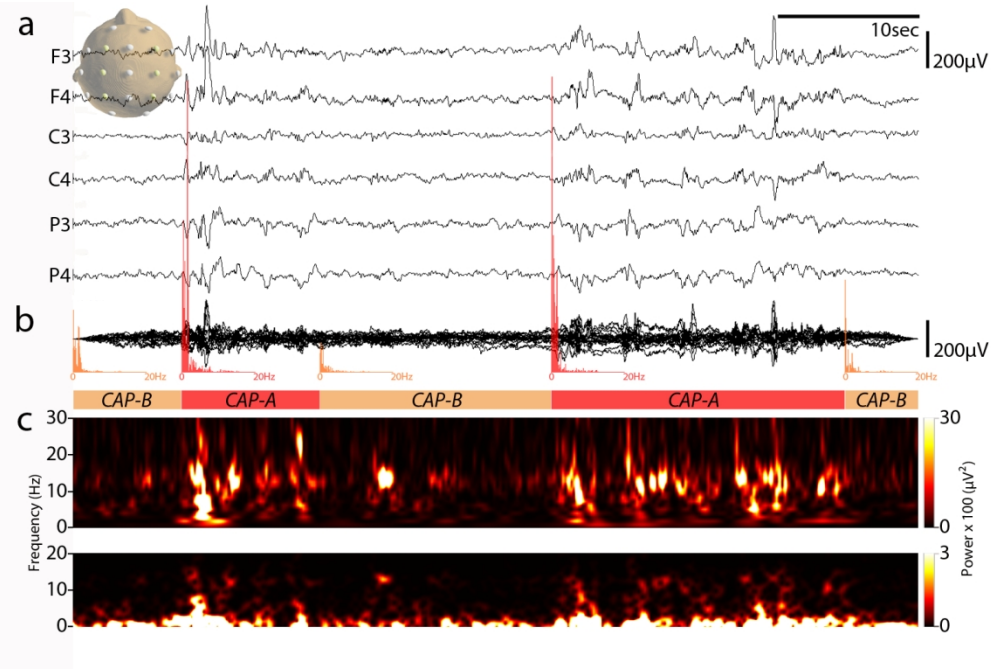

Figure 1. The NREM cyclic alternating pattern (CAP). (a) Sleep EEG with two phases of synchronization standing out of the NREM background. (b) Butterfly plot of all EEG electrodes for the same period, overlaid with cumulative spectral power charts for each scored CAP-A and CAP-B phase. (c) Wavelet and FFT-based time-frequency plots derived from F4 electrode showing the contrast between phases of synchronization (CAP-A) and de-synchronization (CAP-B) in the frequency domain.

135x90mm (300 x 300 DPI)

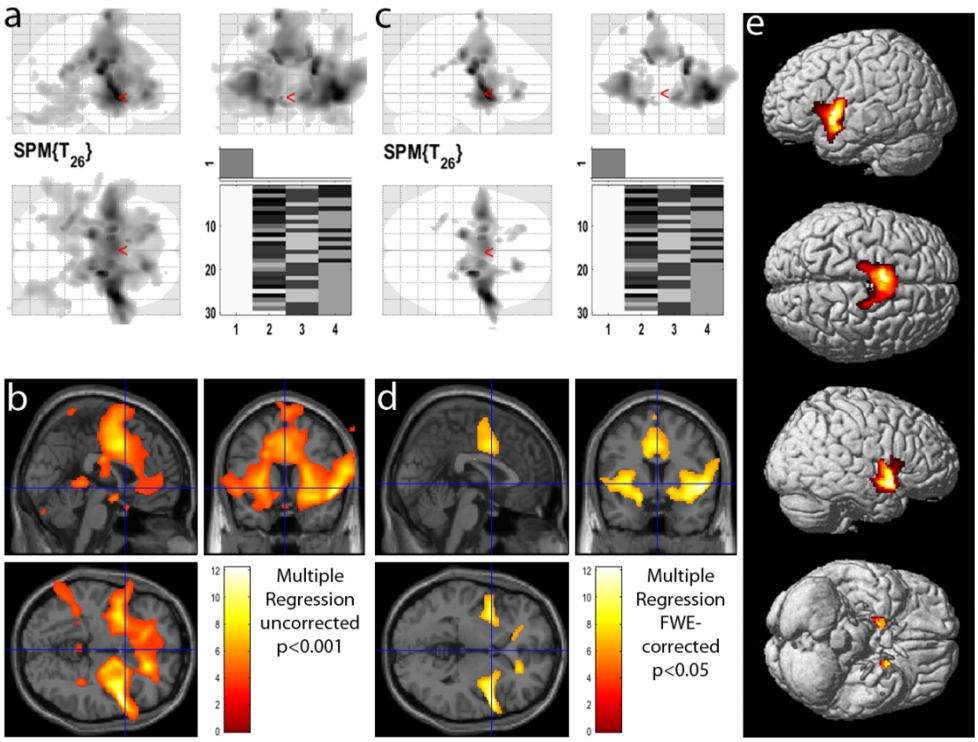

Figure 2. The BOLD correlates of the NREM CAP. (a-d) Glass brain and T1-overlaid uncorrected and corrected contrast maps of group-level analysis corresponding to the CAP-A variable (T subscript denotes degrees of freedom). The design matrix of the multiple regression model for the CAP-A variable (1) is presented, with three regressors for age (2), gender (3) and state (4); the latter referring to the subject been scanned partially sleep deprived or not. Both uncorrected and corrected contrast maps revealed statistically significant changes in BOLD signal bilateral over the insulas (Brodmann area 14/15), the middle cingulate gyrus (Brodmann area 24) and the basal forebrain (Brodmann area 25). (e) 3D surface projection of the corrected contrast clusters.

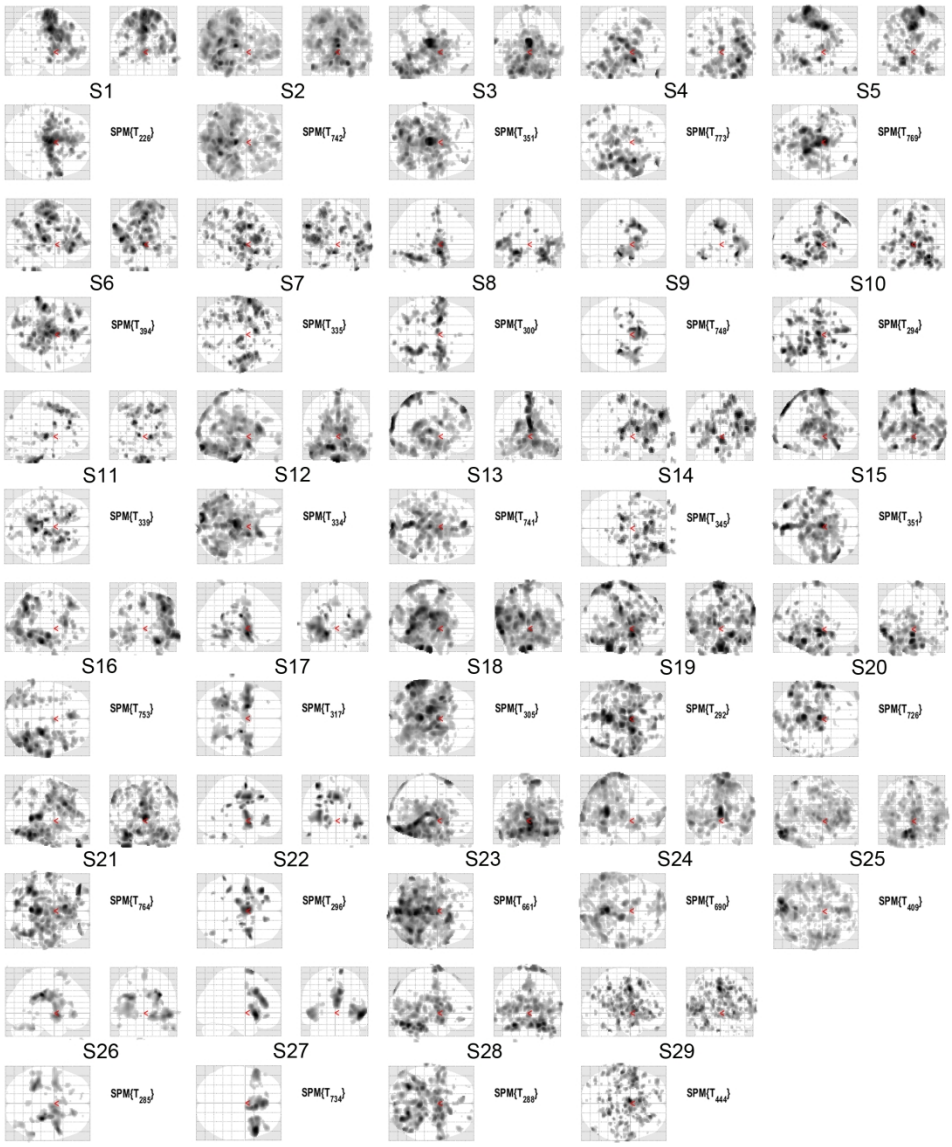

Supplementary Figure 1. Fixed effects analysis CAP-A correlates. Glass brain-overlaid, fixed effects analysis-derived, uncorrected contrast maps of CAP-A synchronization phases from each of the 30 subjects (T subscript denotes degrees of freedom). Notice the high variability of BOLD signal across subjects, that makes the derivation of a common pattern difficult.

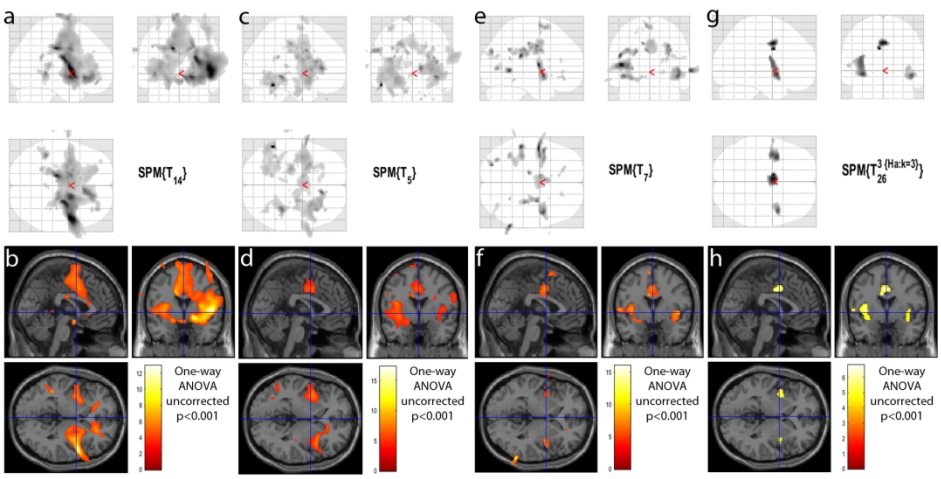

Supplementary Figure 2: Random effects and conjunction analysis across age groups. (a,b) BOLD correlates of the CAP-A synchronization phase for 15 subjects between ages of 10 and 19 years old, projected on glass brain and overlaid on a normalized T1 brain. (c,d) BOLD correlates of the CAP-A synchronization phase for 7 subjects between ages of 20 and 29 years old. (e,f) BOLD correlates of the CAP-A synchronization phase for 8 subjects more than 30 years old. Statistical power can vary between age groups as a result of the different number of participants in each group. (g,h) Conjunction across all 3 age groups.

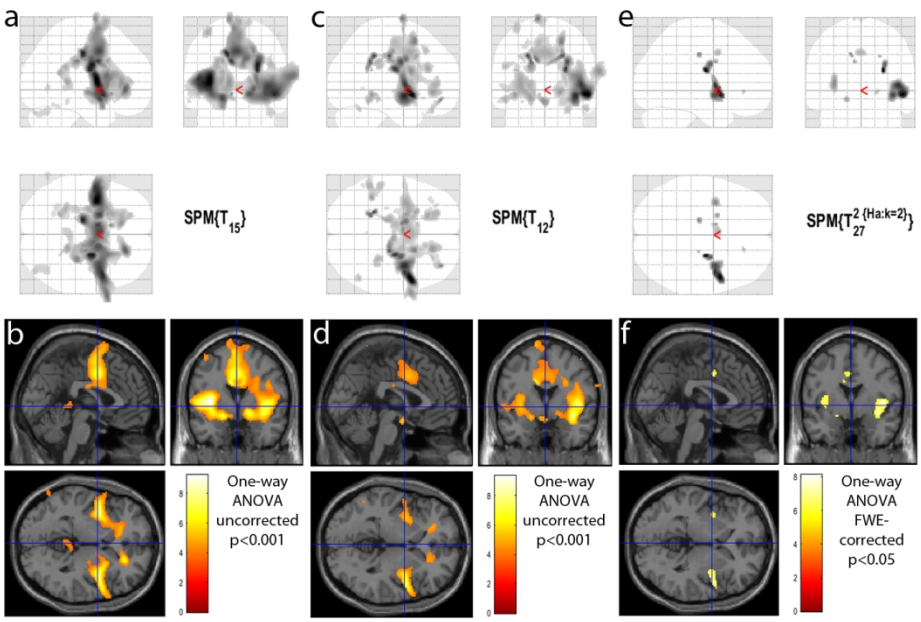

Supplementary Figure 3. Random effects and conjunction analysis across gender groups. (a,b) BOLD correlates of the CAP-A synchronization phase for 16 male subjects, projected on glass brain and overlaid on a normalized T1 brain. (c,d) BOLD correlates of the CAP-A synchronization phase for 14 female subjects. (e,f) Conjunction across the 2 groups.

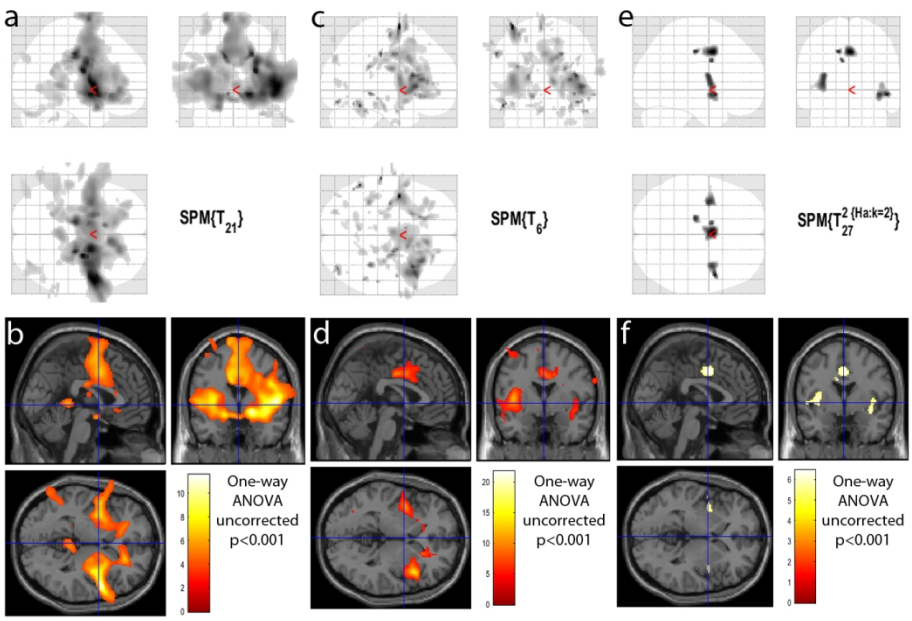

Supplementary Figure 4. Random effects and conjunction analysis across partially sleep-deprived and non sleep-deprived groups. (a,b) BOLD correlates of the CAP-A synchronization phase for 22 partially sleep-deprived subjects, projected on glass brain and overlaid on a normalized T1 brain. (c,d) BOLD correlates of the CAP-A synchronization phase for 8 non sleep-deprived subjects. Statistical power can vary between these groups as a result of the different number of participants in each group. (e,f) Conjunction across the 2 groups.

Figure Legends

Figure 1. The NREM cyclic alternating pattern (CAP). (a) Sleep EEG with two phases of synchronization standing out of the NREM background. (b) Butterfly plot of all EEG electrodes for the same period, overlaid with cumulative spectral power charts for each scored CAP-A and CAP-B phase. (c) Wavelet and FFT-based time-frequency plots derived from F4 electrode showing the contrast between phases of synchronization (CAP-A) and de-synchronization (CAP-B) in the frequency domain.

Figure 2. The BOLD correlates of the NREM CAP. (a-d) Glass brain and T1-overlaid uncorrected and corrected contrast maps of group-level analysis corresponding to the CAP-A variable (T subscript denotes degrees of freedom). The design matrix of the multiple regression model for the CAP-A variable (1) is presented, with three regressors for age (2), gender (3) and state (4); the latter referring to the subject been scanned partially sleep deprived or not. Both uncorrected and corrected contrast maps revealed statistically significant changes in BOLD signal bilateral over the insulas (Brodmann area 14/15), the middle cingulate gyrus (Brodmann area 24) and the basal forebrain (Brodmann area 25). (e) 3D surface projection of the corrected contrast clusters.

Abbreviations

EEG: Electroencephalography / Electroencephalogram

fMRI: Functional magnetic resonance imaging

MRI: Magnetic resonance imaging

CAP: Cyclic alternating pattern

NREM: Non-rapid eye movement

BOLD: blood oxygen-level dependent

EPI: Echo-planar imaging

GLM: General linear model

HRF: Haemodynamic Response Function

FWE: Family-wise error

FDR: False discovery rate

SUPPLEMENTARY MATERIAL

Supplementary Figure Legends

Supplementary Figure 1. Fixed effects analysis CAP-A correlates. Glass brain-overlaid, fixed effects analysis-derived, uncorrected contrast maps of CAP-A synchronization phases from each of the 30 subjects (T subscript denotes degrees of freedom). Notice the high variability of BOLD signal across subjects, that makes the derivation of a common pattern difficult.

Supplementary Figure 2: Random effects and conjunction analysis across age groups. (a,b) BOLD correlates of the CAP-A synchronization phase for 15 subjects between ages of 10 and 19 years old, projected on glass brain and overlaid on a normalized T1 brain. (c,d) BOLD correlates of the CAP-A synchronization phase for 7 subjects between ages of 20 and 29 years old. (e,f) BOLD correlates of the CAP-A synchronization phase for 8 subjects more than 30 years old. Statistical power can vary between age groups as a result of the different number of participants in each group. (g,h) Conjunction across all 3 age groups.

Supplementary Figure 3. Random effects and conjunction analysis across gender groups. (a,b) BOLD correlates of the CAP-A synchronization phase for 16 male subjects, projected on glass brain and overlaid on a normalized T1 brain. (c,d) BOLD correlates of the CAP-A synchronization phase for 14 female subjects. (e,f) Conjunction across the 2 groups.

Supplementary Figure 4. Random effects and conjunction analysis across partially sleep-deprived and non sleep-deprived groups. (a,b) BOLD correlates of the CAP-A synchronization phase for 22 partially sleep-deprived subjects, projected on glass brain and overlaid on a normalized T1 brain. (c,d) BOLD

correlates of the CAP-A synchronization phase for 8 non sleep-deprived subjects. Statistical power can vary between these groups as a result of the different number of participants in each group. (e,f) Conjunction across the 2 groups.

TABLES

Supplementary Table 1. Demographic, pathology/treatment and EEG-fMRI recording data of the selected participants (L: left, R: right, B: bilateral, FLE: frontal lobe epilepsy, PLE: parietal lobe epilepsy, TLE: temporal lobe epilepsy, ILE: insular lobe epilepsy, OLE: occipital lobe epilepsy, JAE: juvenile absence epilepsy, JME: juvenile myoclonic epilepsy, IGE: idiopathic generalized epilepsy, CBZ: carbamazepine, CLM: clobazam, LCM: lacosamide, LEV: levetiracetam, LTG: lamotrigine, OXC: oxcarbazepine, PB: phenobarbital, RUF: rufinamide, TPM: topiramate, VPA: valproic acid, ZNS: zonisamide, *: spontaneous sleep after partial deprivation, SWS: slow wave sleep).

Subjects	Age	Sex	Diagnosis	Anti-epileptic medication	Seizure frequency	Scan time (min)	Total NREM sleep time (min)	NREM Sleep stages	CAP-As
1	12	M	PLE (B)	LEV, OXC, VPA	2-3/day	30	27	I, II, SWS	31
2	30	M	JME	VPA	3-4/year	60	23	I, II	41
3	11	M	OLE (L)	LEV, LTG, OXC, VPA	5-10/day	30	23*	I, II	45
4	14	F	OLE (R)	LCM, LEV, VPA	2-3/week	60	51*	I, II	128
5	24	M	TLE (R)	LEV, OXC,	5-10/month	60	48	I, II, SWS	107

				VPA					
6	11	M	FLE (R)	LEV, VPA	1-3/day	60	33*	I, II, SWS	111
7	16	F	TLE (R)	CBZ, TPM	1-2/week	30	27*	I, II, SWS	45
8	16	M	FLE (L)	CBZ, LEV	3-4/year	60	43*	I, II	56
9	25	F	PLE (B)	CBZ, LEV, VPA, ZNS	15-20/day	60	56*	I, II, SWS	69
10	31	M	TLE (R)	LEV, OXC	1-2/month	60	21	I, II	52
11	11	F	OLE (L)	LEV, RUF	3-5/month	30	24*	I, II, SWS	60
12	38	F	TLE (R)	OXC, TPM	4-10/year	60	53	I, II, SWS	71
13	15	F	FLE (R)	CLM, VPA	10-30/day	60	51*	I, II, SWS	153
14	19	F	TLE (L)	CLM, LEV, OXC	8-20/month	30	26	I, II	57
15	19	M	PLE (R)	LEV, OXC	1-4/day	30	25*	I, II, SWS	49
16	18	F	TLE (R)	LEV, OXC, LCM	2-4/week	60	49*	I, II, SWS	150
17	27	F	FLE (L)	CLM, LCM, TPM, VPA	1-4/week	30	25	I, II, SWS	53

18	35	M	FLE (L)	CBZ, OXC	2-3/week	30	27*	I, II, SWS	50
19	30	M	FLE (R)	CBZ, OXC, ZNS	1-5/week	30	24*	I, II	40
20	20	M	TLE (L)	LEV, OXC	1-4/month	60	49*	I, II, SWS	111
21	17	F	FLE (L)	CBZ, LTG	1-2/month	60	54*	I, II, SWS	218
22	19	M	FLE (L)	LEV, OXC, VPA	3-7/week	60	48*	I, II, SWS	98
23	13	M	IGE	LEV, TPM, VPA	10-30/day	60	51*	I, II, SWS	131
24	42	F	TLE (R)	LEV, OXC	1-2/week	60	42*	I, II, SWS	71
25	13	F	ILE (L)	CBZ, OXC	1-2/month	60	28*	I, II	66
26	27	F	TLE (R)	LEV, OXC, LCM	1-3/week	60	25*	I, II	56
27	35	M	ILE (L)	CLB, LTG, OXC, VPA	10-20/month	60	55*	I, II, SWS	97
28	27	M	FLE (R)	VPA	1/month	60	22*	I, II	38
29	45	M	FLE (R)	OXC, PB	1-6/month	40	28*	I, II, SWS	134

	Total: 1,450	Total: 1,058		Total: 2,388